European Commission | Funding & tender opportunities
Single Electronic Data Interchange Area (SEDIA)

H2020-MSCA-IF-2020

Secure Indoor Communication empowered by Intelligent reflecting Surface (SICIS)

D2.1

Report on joint beamforming optimisation design for security

Authors(s)	Sai Xu, Jie Zhang
Author(s) Affiliation	University of Sheffield, UK
Editor(s):	Sai Xu
Status-Version:	V1.0
Project Number:	101032170
Project Title:	Secure Indoor Communication empowered by Intelligent reflecting Surface
Project Acronym:	SICIS
Work Package Number	2

Abstract

This report pioneers an unprecedented strategy of secure transmission, in which intelligent reflecting surface (IRS) is used as a backscatter device to form and scatter jamming signal while the transmitter (Alice) is regarded as a radio-frequency (RF) source. Specifically, Alice transmits confidential signal to a single-antenna legitimate user (Bob) while the transmission is overheard by multiple single-antenna illegitimate users (Eves). The beamformer at Alice is designed to align with the estimated channel vector from Alice to Bob, in order that the proposed strategy is completely compatible with the common communication system without respect to wiretap. To achieve secure transmission, IRS is deployed to modulate the received confidential signal to jamming signal and reflect it so as to deteriorate the reception at Eves. Based on this model, the reflection coefficient vector of IRS is optimized to minimize the eavesdropped information amount while guaranteeing the reliable communication at Bob. By comparing with the familiar IRS based beamforming scheme and the cooperative jamming scheme in extensive simulations, the feasibility and secrecy performance gain are confirmed for the proposed strategy of IRS-based backscatter jamming.

The results presented in this deliverable have addressed the requirement of Task 2.1 in the SICIS project.

Keywords: Backscatter, beamforming, intelligent reflecting surface (IRS), jamming, physical-layer security (PLS).

Table of Contents

1. INTRODUCTION

Although physical-layer security (PLS) has demonstrated remarkable capacity to secure confidential transmission in radio communications, there is always some inevitable sacrifice of communication performance under the same wireless resource [1], [2]. To compensate, more transmit power is often consumed. With the sixth-generation wireless network (6G) [3] approaching, how to realize high-level resource utilization [4] will become an increasingly major issue. Recent development of intelligent reflecting surface (IRS) opens up new possibilities to PLS, because of its unique merits, such as low power consumption, low cost, flexible deployment, etc [5]. Complied with such a situation, researches on IRS-aided PLS have been thriving [6].

Nevertheless, all these endeavors are restricted to the function of passive relay reflector. To be more specific, IRS is used for the signal enhancement at the legitimate user (Bob) while degrading that at the illegitimate user (Eve), by reflecting the confidential the confidential signal, jamming signal and/or artificial noise (AN) [7]. Different from these conventional methods, this report provides a new approach to applying IRS into PLS, in which IRS-based backscatter communication is exploited. By adjusting the reflection coefficient of elements strategically, IRS is able to modulate the confidential signal from the transmitter (Alice) into jamming signal, thereby deteriorating the reception at Eve for secrecy enhancement. Currently, the implement of PLS is mainly based on the signal quality difference between Bob and Eve, which can be achieved by secure signal processing techniques, including beamforming, AN, cooperative jamming, etc. Through using a good compromise design of beamforming at Alice, the signal quality at Bob and that at Eve can be enhanced and suppressed, respectively [8]. AN and cooperative jamming are another way to secure the transmission, which aim at deteriorating the reception at Eve with little effect on Bob [9]. By combining AN and cooperative jamming with beamforming, the secrecy performance can be improved significantly. Recent breakthroughs in IRS provide PLS with broader researching space. IRS is a programmable digital metasurface, which is perfectly capable of controlling propagation of wireless signals by its unique functionalities of wave absorption, reflection, wave splitting, phase modification, etc [10]. Although the operation of IRS resembles that of relay, IRS reflects the ambient radio-frequency (RF) signals passively rather than transmit new RF signals actively. Moreover, IRS gets out of com plicated signal processing procedure, such as decoding and encoding received information. As a result, the delay, power consumption, cost of IRS are far lower than relay. Recent researches on IRS have revealed that secrecy performance enhancement can be realized by exploiting and controlling wireless propagation. In PLS, the operating principle of IRS is somewhat similar to full-duplex relay [11]. Particularly, IRS is able to help forward confidential signal to Bob for the signal enhancement while alleviating the reception at Eve, by optimizing the amplitude and phase of incoming signal delicately. Additionally, jamming signals or AN can be reflected to disrupt the signal quality at Eve. When channel state information (CSI) of Eve is perfect, IRS-enhanced secure radio systems were investigated in [12] and [13] with only one Bob and one Eve. To address the nonconvex optimization problems, semidefinite relaxation (SDR) was employed to form tractable optimization problems involving beamforming matrices and then the method of Gaussian randomization was adopted to recover a set of approximate solutions of beamforming and reflection coefficient vectors.

When the CSIs of Bob and Eve are imperfect, Yu et al. [7] studied an IRS-aided wireless system, assuming that the line-of-sight (LOS) communication link is blocked. To deteriorate the reception at Eve for security provisioning, AN was also inserted into the transmitted signal at Alice. Then, joint beamformers at Alice and the IRS were optimized to maximize the system sum-rate subject to the maximal information leakage. When the CSI of Eve is completely unknown, Wang et al. [14] presented an IRS-aided secure transmission scheme, in which the power for transmitting confidential

signal is minimized while ensuring the required signal-to-interference -plus-noise ratio (SINR) at Bob, in order to leave more transmit power for AN. Until now, related studies on IRS-based backscatter communication for PLS, however, have not yet started.

Backscatter communication is a passive and green radio technique, through which the transmitter without active RF chains can still send information to its receiver. In new-born ambient backscatter communication (AmBC), for example, the transmitter harvests the existing signal energy scattered in wireless environment to modulate and deliver integrated [16], [17]. In [18], private data from IRS was backscattered along with enhancement of primary communication. In [19], the probability was deduced approximately that the channel of backscatter communication is better than the direct one in IRS-based backscatter communication. In [20], IRS was integrated into cognitive radio (CR) communication system, so as to strengthen the primary communication as well as to realize backscatter transmission.

IRS-based backscatter communication is a highly promising technique owing to its low power consumption and high-level reuse rate of spectrum. However, the technique has not ever been exploited for PLS. Motivated by this, we investigates a novel secure transmission strategy of IRS-based backscatter jamming. Compared to the conventional IRS-aided PLS scheme, the proposed strategy has many advantages: 1) the original design of communication system is allowed to remain unchanged when IRS is plugged to enhance secrecy; 2) when jamming signal is employed to deteriorate the reception at Eve, it is unnecessary to add the module of jamming signal into the transmitter; and 3) when the power is limited at Alice and the signal is designed entirely towards Bob, the secrecy can still be realized by deploying IRS. Distinguished from the scheme of cooperative jamming, IRS-based backscatter communication requires no additional jamming power. The main contributions made by this report are outlined as follows.

1) To the best of our knowledge, it is the initial attempt to apply IRS-based backscatter into PLS. This report proposes to employ IRS to harvest the energy of confidential signal from Alice in order to generate jamming signal for security provisioning for the first time. In this strategy, the beamformer at Alice is designed to align with the estimated Alice-Bob channel vector and all transmit power is used to send confidential signal. To secure the transmission, IRS is deployed to modulate the received confidential signal into jamming signal by adjusting the reflection coefficient of elements strategically, so as to deteriorate the reception at Eves. Such a secure design enables the compatibility with the common communication system without respect to wiretap.

2) This report formulates two optimization problems in the cases of perfect and imperfect CSI to maximize the secrecy while guaranteeing the reliable communication at Bob. Specifically, when CSI is perfect, the coefficient of each element at the IRS is designed to minimize the maximum SINR of Eves under the constraint of SINR at Bob. When CSI is imperfect with Gaussian channel errors assumed, the passive beamforming aims to minimize the outage SINR of Eves under the constraints of outage SINR probabilities at Bob and Eves.

3) This report addresses the above two optimization problems. What is more, the complexity analyses are presented for the proposed schemes. Then, the proposed strategy is compared with the conventional IRS-aided PLS scheme and the cooperative jamming scheme by simulations, confirming the feasibility and secrecy performance gain of IRS-based backscatter jamming.

2. SYSTEM MODEL

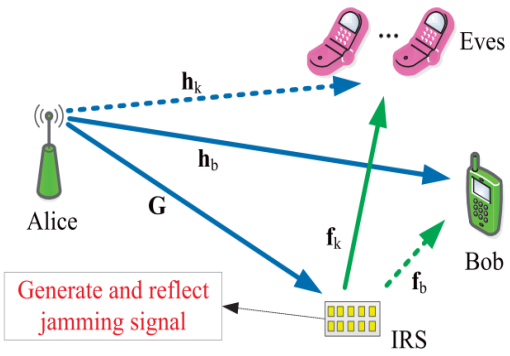

Fig. 1. Illustration of secure transmission via IRS-based backscatter jamming.

We show a model of secure transmission via IRS-based backscatter jamming in Fig. 1, where an N-antenna Alice intends to send the signal bearing confidential information to Bob with single antenna while the transmission is overheard by K Eves with single antenna. To enhance security without or with little compromise of the signal quality at Bob, the beamforming vector at Alice is designed to align with the channel from Alice to Bob, while an IRS comprising L elements is employed to secure the transmission. Different from the existing IRS-aided PLS methods, the incident signal is remodulated as jamming signal at the IRS when reflected. In the model, the IRS fulfills two main functions through the tactical and real-time adjustment of its elements' reflection coefficient. In other words, the incident signal turns into random jamming signal and is reflected simultaneously, with well-designed antenna power. The whole reflection process seems as if the IRS reflects the same-power jamming signal as the received confidential signal via passive beamforming. Clearly, the purpose of deploying the IRS here is to interfere with the reception at Eve rather than reduce its received signal strength. Since the IRS operates with low power consumption, the total power budget of the whole system is hardly increased. Beyond all doubt, the deployment of IRS provides a powerful way of green interference. Assuming that the states of all channels change slowly and only considering the first IRS reflection, the signals at Bob and Eves are, respectively, given by

$$y_b = \mathbf{h}_b^H \mathbf{w} s + \mathbf{f}_b^H \mathbf{z} + n_b$$
$$y_k = \mathbf{h}_k^H \mathbf{w} s + \mathbf{f}_k^H \mathbf{z} + n_k, \ k \in \mathcal{K}$$

The SINRs at Bob and Eve are given by

$$\gamma_b = \frac{\left|\mathbf{h}_b^H \mathbf{w}\right|^2}{\sigma_b^2 + \left|\mathbf{f}_b^H \mathbf{\Omega G w}\right|^2}$$
$$\gamma_k = \frac{\left|\mathbf{h}_k^H \mathbf{w}\right|^2}{\sigma_e^2 + \left|\mathbf{f}_k^H \mathbf{\Omega G w}\right|^2}, \ k \in \mathcal{K}.$$

We consider the transmission designs in two cases of perfect and imperfect CSIs.

2.1. Minimizing SINR at Eve With Perfect CSI

Define If all involved $\boldsymbol{\theta} = \left[\beta_1 e^{j\theta_1}, \beta_2 e^{j\theta_2}, \ldots, \beta_L e^{j\theta_L}\right]^H$. CSIs are perfect, this report will minimize the maximum SINR of Eves under the constraint of SINR at Bob, which is formulated as follows:

$$(\mathcal{P}1.1) \quad \min_{\boldsymbol{\theta}} \ \max_{k\in\mathcal{K}} \ \gamma_k$$
$$\text{s.t.} \ \ \gamma_b \geq \Gamma_b$$
$$\beta_l \leq 1, 0 \leq \theta_l \leq 2\pi \quad \forall l \in \mathcal{L}$$

where Γ_b denotes the SINR floor for guaranteeing the reliable communication at Bob.

2.2. Minimizing Outage SINR at Eve With Imperfect CSI

If all involved CSIs are imperfect with their estimation error obeying Gaussian distribution, this report will minimize the outage SINR of Eves under the constraints of outage SINR probabilities at Bob and Eves, which is formulated as

$$(\mathcal{P}2.1) \quad \min_{\boldsymbol{\theta}} \ \Gamma_e$$
$$\text{s.t.} \ \ \Pr\{\gamma_d \leq \Gamma_d\} \leq \varepsilon_b \qquad (1)$$
$$\Pr\left\{\max_{k\in\mathcal{K}} \gamma_k - \Gamma_e \leq 0\right\} \geq 1-\varepsilon_e \qquad (2)$$
$$\beta_l \leq 1, 0 \leq \theta_l \leq 2\pi \quad \forall l \in \mathcal{L}.$$

In problem (P2.1), Γ_d and Γ_e are the outage SINRs at Bob and Eves subject to their SINR outage probabilities, respectively. $\varepsilon b \in (0,1)$and $1-\varepsilon e \in (0,1)$denote the required thresholds of SINR outage probability at Bob and Eves, respectively. Clearly, (1) can limit the SINR at Bob below d with an acceptable upper limit of probability εb, while (2) is used to guarantee the SINRs at Eves below Γ_e with an acceptable lower limit of probability $1-\varepsilon e$.

3. BEAMFORMING OPTIMIZATION WITH PERFECT CSI

This section will optimize the beamforming design to minimize the maximum SINR of Eves under the constraint of SINR at Bob in the case of perfect CSI. Problem (P1.1) is nonconvex, thus being difficult to solve directly. In view of this, we transform this problem into a tractable convex problem by lifting it into a high dimension and dropping the rank-one constraint based on SDR. Then, the existing CVX solvers are employed to address the formed new problem, followed by the recovery of an approximate rank-one solution through the standard Gaussian randomization method. Finally, the complexity analysis of the algorithm is given. Specifically, a slack variable e is introduced and problem (P1.1) translates into the following form:

$$\min_{\boldsymbol{\theta}} \ \Gamma_e$$
$$\text{s.t.} \ \ \gamma_b \geq \Gamma_b$$
$$\max_{k\in\mathcal{K}} \gamma_k \leq \Gamma_e$$
$$\beta_l \leq 1, 0 \leq \theta_l \leq 2\pi \quad \forall l \in \mathcal{L}.$$

4.

It is easy to find that the constraint max $k \in K\gamma k \leq e$ is equivalent to $\gamma k \leq e \, \forall k \in K$. Moreover, the constraint $\beta_l \leq 1, 0 \leq \theta_l \leq 2\pi$ can be rewritten as a unit-modulus constraint $|\theta_l| \leq 1$. Thus, this problem is reformulated as:

$$\begin{aligned}
\min_{\boldsymbol{\theta}} \quad & \Gamma_e \\
\text{s.t.} \quad & \frac{\left|\mathbf{h}_b^H \mathbf{w}\right|^2}{\sigma_b^2 + \left|\boldsymbol{\theta}^H \boldsymbol{\Phi}_b\right|^2} \geq \Gamma_b \\
& \frac{\left|\mathbf{h}_k^H \mathbf{w}\right|^2}{\sigma_e^2 + \left|\boldsymbol{\theta}^H \boldsymbol{\Phi}_k\right|^2} \leq \Gamma_e \quad \forall k \in \mathcal{K} \\
& |\theta_l| \leq 1 \quad \forall l \in \mathcal{L}.
\end{aligned}$$

Let $\boldsymbol{\Phi}_b = \text{diag}\left(\mathbf{f}_b^H\right)\mathbf{G}\mathbf{w} and \boldsymbol{\Phi}_k = \text{diag}\left(\mathbf{f}_k^H\right)\mathbf{G}\mathbf{w}.$ Then, it is easily derived that $\mathbf{f}_b^H \boldsymbol{\Omega}\mathbf{G}\mathbf{W} = \boldsymbol{\theta}^H \boldsymbol{\Phi}_b and \mathbf{f}_k^H \boldsymbol{\Omega}\mathbf{G}\mathbf{w} = \boldsymbol{\theta}^H \boldsymbol{\Phi}_k$ This problem is further expressed as：

$$\begin{aligned}
\min_{\boldsymbol{\theta}} \quad & \Gamma_e \\
\text{s.t.} \quad & \frac{\left|\mathbf{h}_b^H \mathbf{w}\right|^2}{\sigma_b^2 + \left|\boldsymbol{\theta}^H \boldsymbol{\Phi}_b\right|^2} \geq \Gamma_b \\
& \frac{\left|\mathbf{h}_k^H \mathbf{w}\right|^2}{\sigma_e^2 + \left|\boldsymbol{\theta}^H \boldsymbol{\Phi}_k\right|^2} \leq \Gamma_e \quad \forall k \in \mathcal{K} \\
& |\theta_l| \leq 1 \quad \forall l \in \mathcal{L}.
\end{aligned}$$

Using SDR and removing the constraint rank(θ) = 1, the problem is relaxed as：

$$\begin{aligned}
(\mathcal{P}1.2) \quad \min_{\boldsymbol{\Theta}} \quad & \Gamma_e \\
\text{s.t.} \quad & \boldsymbol{\Phi}_b^H \boldsymbol{\Theta} \boldsymbol{\Phi}_b \leq \Upsilon_b \\
& \boldsymbol{\Phi}_k^H \boldsymbol{\Theta} \boldsymbol{\Phi}_k \geq \Upsilon_k \quad \forall k \in \mathcal{K} \\
& \boldsymbol{\Theta}_{l,l} \leq 1, \ l \in \mathcal{L} \\
& \boldsymbol{\Theta} \succeq \mathbf{0}.
\end{aligned}$$

5.

Since the beamforming vector $\mathbf{w}$ is designed to align with the channel $\mathbf{h_b}$, we have $\mathbf{w} = (\mathbf{h}b/|\mathbf{h}b|)$. This relaxed problem is convex semidefifinite program (SDP) problem and easily solved by many existing SDP solvers. Generally, the solution to this relaxed problem may not be of rank-one. In this case, an approximate rank-one solution $\boldsymbol{\theta}$ $*$ to the original optimization problem (P1.1) can be recovered through the standard Gaussian randomization method [31].

6. BEAMFORMING OPTIMIZATION WITH IMPERFECT CSI

This section will optimize the beamforming design to minimize the outage SINR of Eves under the constraints of outage SINR probabilities at Bob and Eves in the case of imperfect CSI. Compared to problem (P1.1), it is tougher to directly solve problem (P2.1), because the closed-form expressions for the probabilistic constraints (1) and (2) are not available. Facing such a challenge, problem (P2.1) is firstly replaced with a high-dimension optimization problem. Then, the probabilistic constraints are transformed into their approximate deterministic form by two conservative and approximate approaches, respectively. Next, a possible suboptimal solution is obtained by dropping the rank-one constraint, followed by the recovery of an approximate rank-one solution through the standard Gaussian randomization method. Finally, the complexity analysis of the algorithm is given. Since the

channel information is imperfect, the beamforming vector w is designed to align with $\overline{hb}$ with w = ($\overline{hb}$/|$\overline{hb}$|). In problem (P2.1), it is easily observed that:

$$\gamma_b \geq \Gamma_b \Longleftrightarrow \frac{\left|\mathbf{h}_b^H \mathbf{w}\right|^2}{\sigma_b^2 + \left|\boldsymbol{\theta}^H \boldsymbol{\Phi}_b\right|^2} \geq \Gamma_b \tag{3}$$

$$\max_{k\in\mathcal{K}} \gamma_k \leq \Gamma_e \Longleftrightarrow \max_{k\in\mathcal{K}} \frac{\left|\mathbf{h}_k^H \mathbf{w}\right|^2}{\sigma_e^2 + \left|\boldsymbol{\theta}^H \boldsymbol{\Phi}_k\right|^2} \leq \Gamma_e. \tag{4}$$

By making change of variables:

$$\eta_b = \begin{bmatrix} \mathbf{h}_b \\ \boldsymbol{\Phi}_b \end{bmatrix}, \hat{\Theta}_b = \begin{bmatrix} \mathbf{W} & 0 \\ 0 & -\Gamma_b \boldsymbol{\Theta} \end{bmatrix} \quad \eta_k = \begin{bmatrix} \mathbf{h}_k \\ \boldsymbol{\Phi}_k \end{bmatrix}, \hat{\Theta}_e = \begin{bmatrix} \mathbf{W} & 0 \\ 0 & -\Gamma_e \boldsymbol{\Theta} \end{bmatrix}$$

where $Y_k = ([|\bar{\mathbf{h}}_k^H \mathbf{w}|^2]/\Gamma_e) - \sigma_e^2$ and $\boldsymbol{\eta}_b \sim \mathrm{CN}\left(\mathbf{0}, \boldsymbol{\Sigma}_b\right)$, $\boldsymbol{\eta}_k \sim \mathrm{CN}\left(\mathbf{0}, \boldsymbol{\Sigma}_k\right)$. Thus, (3) and (4) can be rewritten as:

$$\gamma_b \geq \Gamma_b \Longleftrightarrow \boldsymbol{\eta}_b^H \hat{\boldsymbol{\Theta}}_b \boldsymbol{\eta}_b \geq \sigma_b^2 \Gamma_b \tag{5}$$

$$\max_{k\in\mathcal{K}} \gamma_k \leq \Gamma_e \Longleftrightarrow \max_{k\in\mathcal{K}} \boldsymbol{\eta}_k^H \hat{\boldsymbol{\Theta}}_e \boldsymbol{\eta}_k \leq \sigma_e^2 \Gamma_e. \tag{6}$$

Substituting (5) and (6) into (1) and (2), problem (P2.1) is reformulated as:

$$\begin{aligned} \min_{\boldsymbol{\Theta}} \quad & \Gamma_e \\ \text{s.t.} \quad & \Pr\left\{\boldsymbol{\eta}_b^H \hat{\boldsymbol{\Theta}}_b \boldsymbol{\eta}_b \geq \sigma_b^2 \Gamma_b\right\} \geq 1 - \varepsilon_b \\ & \Pr\left\{\max_{k\in\mathcal{K}} \boldsymbol{\eta}_k^H \hat{\boldsymbol{\Theta}}_e \boldsymbol{\eta}_k \leq \sigma_e^2 \Gamma_e\right\} \geq 1 - \varepsilon_e \\ & \boldsymbol{\Theta}_{l,l} \leq 1, \ l \in \mathcal{L} \\ & \boldsymbol{\Theta} \succeq \mathbf{0}, \operatorname{rank}(\boldsymbol{\Theta}) = 1 \end{aligned}$$

Using SDR and removing the constraint rank($\boldsymbol{\Theta}$)= 1, the problem is relaxed as:

$$\begin{aligned} \min_{\boldsymbol{\Theta}} \quad & \Gamma_e \\ \text{s.t.} \quad & \Pr\left\{\boldsymbol{\eta}_b^H \hat{\boldsymbol{\Theta}}_b \boldsymbol{\eta}_b \geq \sigma_b^2 \Gamma_b\right\} \geq 1 - \varepsilon_b \\ & \Pr\left\{\max_{k\in\mathcal{K}} \boldsymbol{\eta}_k^H \hat{\boldsymbol{\Theta}}_e \boldsymbol{\eta}_k \leq \sigma_e^2 \Gamma_e\right\} \geq 1 - \varepsilon_e \qquad (7) \\ & \boldsymbol{\Theta}_{l,l} \leq 1, \ l \in \mathcal{L} \\ & \boldsymbol{\Theta} \succeq \mathbf{0}. \end{aligned}$$

For constraint (7), it can be relaxed as:

$$\Pr\left\{\boldsymbol{\eta}_k^H \hat{\boldsymbol{\Theta}}_e \boldsymbol{\eta}_k \leq \sigma_e^2 \Gamma_e\right\} \geq 1 - \varepsilon_k \quad \forall k \in \mathcal{K} \tag{8}$$

where εk = 1 − (1 − εe)1/K. The reason is:

$$(8) \Longrightarrow \prod_{k=1}^{K} \Pr\left\{\boldsymbol{\eta}_k^H \hat{\boldsymbol{\Theta}}_e \boldsymbol{\eta}_k \le \sigma_e^2 \Gamma_e\right\} \ge 1-\varepsilon_e \Longleftrightarrow (7).$$

Thus, problem (P2.1) is relaxed as

$$\begin{aligned}
(\mathcal{P}2.2) \quad & \min_{\boldsymbol{\Theta}} \ \Gamma_e \\
& \text{s.t. } \Pr\left\{\boldsymbol{\eta}_b^H \hat{\boldsymbol{\Theta}}_b \boldsymbol{\eta}_b \ge \sigma_b^2 \Gamma_b\right\} \ge 1-\varepsilon_b \qquad (9) \\
& \quad \Pr\left\{\boldsymbol{\eta}_k^H \hat{\boldsymbol{\Theta}}_e \boldsymbol{\eta}_k \le \sigma_e^2 \Gamma_e\right\} \ge 1-\varepsilon_k \\
& \qquad\qquad \forall k \in \mathcal{K} \qquad (10) \\
& \quad \boldsymbol{\Theta}_{l,l} \le 1, \ l \in \mathcal{L} \\
& \quad \boldsymbol{\Theta} \succeq \mathbf{0}.
\end{aligned}$$

To address this problem, the probabilistic constraints need to be transformed into their corresponding deterministic form. The following sections will present two approaches to make the conversions. The first one is named as the ellipsoid bounding approach and the second one is the Bernstein-type equality approach.

6.1. Conversion Using Ellipsoid Bounding Approach

According to the property of Gaussian random variable, probabilistic uncertainties can be removed. Instead, the constraints of spherical uncertainties are formed. To be specific, the considered channels are imperfect and the estimation errors all obey Gaussian distribution. Thus, $\boldsymbol{\eta}_b$ consists of the deterministic $\bar{\boldsymbol{\eta}}_b$ and the random $\boldsymbol{\eta}_b$ $\boldsymbol{\eta}_k$ is composed of the deterministic $\bar{\boldsymbol{\eta}}_k$ and the random $\boldsymbol{\eta}_k$, with

$$\tilde{\eta}_b \sim \mathcal{CN}(\mathbf{0}, \boldsymbol{\Sigma}_b), \quad \tilde{\eta}_k \sim \mathcal{CN}(\mathbf{0}, \boldsymbol{\Sigma}_k).$$

Therefore, it can be deduced that $\boldsymbol{\eta}_b$ is inside $2(\mathrm{L}+\mathrm{N})$ dimensional ellipsoid region with the probability

$$\Pr\{\tilde{\boldsymbol{\eta}}_b \in \mathcal{R}_b\} = 1-\varepsilon_b$$

where

$$r_b = \sqrt{\frac{\Phi^{-1}(1-\varepsilon_b)}{2}}.$$

In this equation, Φ^{-1} is the inverse cumulative density function (CDF) of the χ^2 random distribution with $2(L+N)$ degrees of freedom and normalized variance. Similarly, it can be deduced that $\boldsymbol{\eta}_k$ is inside a $2(L+N)$-dimensional ellipsoid region with the probability

$$\Pr\{\tilde{\boldsymbol{\eta}}_k \in \mathcal{R}_k\} = 1-\varepsilon_k$$

where $\mathrm{R}_k = \{\boldsymbol{\eta}_k : \boldsymbol{\eta}_k^H \boldsymbol{\Sigma}_k^{-1} \boldsymbol{\eta}_k \le r_k^2\}$ represents the ellipsoid region. r_k denotes the ellipsoid region. r_k restricts the scope of R_k, which is given by:

$$r_k = \sqrt{\frac{\Phi^{-1}(1-\varepsilon_k)}{2}}.$$

Based on these discussions, it can be easily deduced that:

$$\begin{aligned}
&\boldsymbol{\eta}_b^H \hat{\boldsymbol{\Theta}}_b \boldsymbol{\eta}_b \ge \sigma_b^2 \Gamma_b \quad \forall \tilde{\boldsymbol{\eta}}_b \in \mathcal{R}_b \Longrightarrow (9).\\
&\boldsymbol{\eta}_k^H \hat{\boldsymbol{\Theta}}_e \boldsymbol{\eta}_k \le \sigma_e^2 \Gamma_e \quad \forall \tilde{\boldsymbol{\eta}}_k \in \mathcal{R}_k \Longrightarrow (10).
\end{aligned}$$

Therefore, problem (P2.2) translates into the problem of worst case robust minimization under the spherical bounding constraints conservatively and approximately as follows:

$$\begin{aligned}
\min_{\boldsymbol{\Theta}} \quad & \Gamma_e \\
\text{s.t.} \quad & \boldsymbol{\eta}_b^H \hat{\boldsymbol{\Theta}}_b \boldsymbol{\eta}_b \ge \sigma_b^2 \Gamma_b \quad \forall \tilde{\boldsymbol{\eta}}_b \in \mathcal{R}_b \\
& \boldsymbol{\eta}_k^H \hat{\boldsymbol{\Theta}}_e \boldsymbol{\eta}_k \le \sigma_e^2 \Gamma_e \quad \forall \tilde{\boldsymbol{\eta}}_k \in \mathcal{R}_k,\ k \in \mathcal{K} \\
& \boldsymbol{\Theta}_{l,l} \le 1,\ l \in \mathcal{L} \\
& \boldsymbol{\Theta} \succeq 0.
\end{aligned}$$

According to the S -procedure [32] this beamforming optimization problem can be reformulated as:

$$\begin{aligned}
(\mathcal{P}2.3) \quad \min_{\boldsymbol{\Theta}} \quad & \Gamma_e \\
\text{s.t.} \quad & \begin{bmatrix} \lambda_b \boldsymbol{\Sigma}_b^{-1} + \hat{\boldsymbol{\Theta}}_b & \hat{\boldsymbol{\Theta}}_b \bar{\boldsymbol{\eta}}_b \\ \bar{\boldsymbol{\eta}}_b^H \hat{\boldsymbol{\Theta}}_b & \bar{\boldsymbol{\eta}}_b^H \hat{\boldsymbol{\Theta}}_b \bar{\boldsymbol{\eta}}_b - \sigma_b^2 \Gamma_b - \lambda_b r_b^2 \end{bmatrix} \\
& \quad \succeq \mathbf{0} \\
& \begin{bmatrix} \lambda_k \boldsymbol{\Sigma}_k^{-1} - \hat{\boldsymbol{\Theta}}_e & -\hat{\boldsymbol{\Theta}}_e \bar{\boldsymbol{\eta}}_k \\ -\bar{\boldsymbol{\eta}}_k^H \hat{\boldsymbol{\Theta}}_e & \sigma_e^2 \Gamma_e - \bar{\boldsymbol{\eta}}_k^H \hat{\boldsymbol{\Theta}}_e \bar{\boldsymbol{\eta}}_k - \lambda_k r_k^2 \end{bmatrix} \\
& \quad \succeq \mathbf{0},\ k \in \mathcal{K} \\
& \lambda_b \ge 0,\ \lambda_k \ge 0,\ k \in \mathcal{K} \\
& \boldsymbol{\Theta}_{l,l} \le 1,\ l \in \mathcal{L} \\
& \boldsymbol{\Theta} \succeq \mathbf{0}.
\end{aligned}$$

When Γ_e is fixed, this problem (P2.3) is a convex SDP problem and easily solved by many existing CVX solvers. Thus, the optimal Γ_e can be obtained by jointly employing CVX solvers and the bisection method. However, this is not a cost-efficient way to solve problem (P2.2). The main reasons are: 1) the accuracy of the direct channel estimation is far higher than that of the cascaded channels; 2) the accuracy of the direct channel estimation does not have much effect on the proposed scheme; 3) due to the path loss from the IRS to Bob and Eve, the amplitudes of the direct channels differ hugely from those of the cascaded channels by orders of magnitude; and 4) the aforementioned solving method for problem(P2.3)has high computation complexity. In view of these reasons, we adopt the degraded form of problem(P2.3). Specifically, the right-hand side of(5) and (6)are replaced with

$$\mathbf{\Phi}_b^H \mathbf{\Theta} \mathbf{\Phi}_b \le \Upsilon_b$$
$$\max_{k\in\mathcal{K}} \mathbf{\Phi}_k^H \mathbf{\Theta} \mathbf{\Phi}_k \ge \Upsilon_k$$

where $\Upsilon_b = ([|\bar{\mathbf{h}}_b^H \mathbf{w}|^2]/\Gamma_b) - \sigma_b^2$ and $\Upsilon_k = ([|\bar{\mathbf{h}}_k^H \mathbf{w}|^2]/\Gamma_e) - \sigma_e^2$. The meanings of other symbols are given in Section III. In this case, similar to the conversion (P2.2) to (P2.3), problem (P2.2) can also translate into the following form:

$$\begin{aligned}
(\mathcal{P}2.4)\quad \min_{\mathbf{\Theta}}\quad & \Gamma_e \\
\text{s.t.}\quad & \begin{bmatrix} \lambda_b \mathbf{R}_b^{-1} - \mathbf{\Theta} & -\mathbf{\Theta}_b \bar{\mathbf{\Phi}}_b \\ -\bar{\mathbf{\Phi}}_b^H \mathbf{\Theta} & \Upsilon_b - \bar{\mathbf{\Phi}}_b^H \mathbf{\Theta}_b \bar{\mathbf{\Phi}}_b - \lambda_b d_b^2 \end{bmatrix} \\
& \quad \succeq \mathbf{0} \\
& \begin{bmatrix} \lambda_k \mathbf{R}_k^{-1} + \mathbf{\Theta}_e & \mathbf{\Theta}_e \bar{\mathbf{\Phi}}_k \\ \bar{\mathbf{\Phi}}_k^H \mathbf{\Theta}_e & \bar{\mathbf{\Phi}}_k^H \mathbf{\Theta}_e \bar{\mathbf{\Phi}}_k - \Upsilon_e - \lambda_k d_k^2 \end{bmatrix} \\
& \quad \succeq \mathbf{0},\ k \in \mathcal{K} \\
& \lambda_b \ge 0,\ \lambda_k \ge 0,\ k \in \mathcal{K} \\
& \mathbf{\Theta}_{l,l} \le 1,\ l \in \mathcal{L} \\
& \mathbf{\Theta} \succeq \mathbf{0}.
\end{aligned}$$

In this problem, the symbols $\mathbf{R}_b$, $\mathbf{R}_k$, λ_b, and λ_k have similar meanings as $\mathbf{\Sigma}_b$ $\mathbf{\Sigma}_k$,rb, and rk in (P2.3). Generally, the solution to this relaxed problem may be not of rank-one. In this case, an approximate rank-one solution $\theta*$ to the original optimization problem (P2.1) can be recovered through the standard Gaussian randomization method [31].

6.2. Conversion Using Bernstein-Type Inequality Approach

As mentioned above, $\boldsymbol{\eta}_b$ consists of the deterministic $\bar{\boldsymbol{\eta}}_b$ and the random $\tilde{\boldsymbol{\eta}}_b$; $\boldsymbol{\eta}_k$ is composed of the deterministic $\bar{\boldsymbol{\eta}}_k$ and the random $\tilde{\boldsymbol{\eta}}_k$,with:

$$\tilde{\boldsymbol{\eta}}_b \sim \mathcal{CN}(\mathbf{0}, \mathbf{\Sigma}_b), \quad \tilde{\boldsymbol{\eta}}_k \sim \mathcal{CN}(\mathbf{0}, \mathbf{\Sigma}_k).$$

Thus, $\boldsymbol{\eta}_b^H \mathbf{\Omega}_b \boldsymbol{\eta}_b$ can be rewritten as:

$$\begin{aligned}
\boldsymbol{\eta}_b^H \hat{\mathbf{\Theta}}_b \boldsymbol{\eta}_b =& (\bar{\boldsymbol{\eta}}_b + \tilde{\boldsymbol{\eta}}_b)^H \hat{\mathbf{\Theta}}_b (\bar{\boldsymbol{\eta}}_b + \tilde{\boldsymbol{\eta}}_b) \\
=& \bar{\boldsymbol{\eta}}_b^H \hat{\mathbf{\Theta}}_b \bar{\boldsymbol{\eta}}_b + \tilde{\boldsymbol{\eta}}_b^H \hat{\mathbf{\Theta}}_b \tilde{\boldsymbol{\eta}}_b + 2\mathrm{Re}\left(\bar{\boldsymbol{\eta}}_b^H \hat{\mathbf{\Theta}}_b \bar{\boldsymbol{\eta}}_b\right) \\
\boldsymbol{\eta}_k^H \hat{\mathbf{\Theta}}_e \boldsymbol{\eta}_k =& \bar{\boldsymbol{\eta}}_k^H \hat{\mathbf{\Theta}}_e \bar{\boldsymbol{\eta}}_k + \tilde{\boldsymbol{\eta}}_k^H \hat{\mathbf{\Theta}}_e \tilde{\boldsymbol{\eta}}_k + 2\mathrm{Re}\left(\bar{\boldsymbol{\eta}}_k^H \hat{\mathbf{\Theta}}_e \bar{\boldsymbol{\eta}}_k\right).
\end{aligned}$$

Then, constraint (9) is rewritten as

$$\Pr\left\{\mathbf{x}_b^H \mathbf{\Lambda}_b \mathbf{x}_b + 2\mathrm{Re}\left(\mathbf{x}_b^H \mathbf{a}_b\right) \le c_b\right\} \le \varepsilon_b \qquad (11)$$

where $\mathbf{x}_b \sim \mathrm{CN}(0, \mathbf{I}_{(L+N)})$ and

$$
\begin{aligned}
c_b &= \sigma_b^2\Gamma_b - \bar{\boldsymbol{\eta}}_b^H\hat{\boldsymbol{\Theta}}_b\bar{\boldsymbol{\eta}}_b \\
\boldsymbol{\Lambda}_b &= \boldsymbol{\Sigma}_b^{1/2}\hat{\boldsymbol{\Theta}}_b\boldsymbol{\Sigma}_b^{1/2} \\
\mathbf{a}_b &= \boldsymbol{\Sigma}_b^{1/2}\hat{\boldsymbol{\Theta}}_b\bar{\boldsymbol{\eta}}_b.
\end{aligned}
$$

The probabilistic constraint(9)can be transformed into its deterministic form conservatively as follows:

$$
\mathrm{Tr}(\boldsymbol{\Lambda}_b) - \sqrt{2\kappa_b}\sqrt{\|\mathrm{vec}(\boldsymbol{\Lambda}_b)\|^2 + 2\|\mathbf{a}_b\|^2} - \kappa_b s^-(\boldsymbol{\Lambda}_b) \geq c_b \tag{12}
$$

where $\kappa_b = -\ln(\varepsilon_b)$ That is to say, if (12) is tenable, then constraint (9) also holds true.

$$
\Pr\left\{\mathbf{x}_k^H\boldsymbol{\Lambda}_k\mathbf{x}_k + 2\mathrm{Re}\left(\mathbf{x}_k^H\mathbf{a}_k\right) \geq c_k\right\} \leq \varepsilon_k \quad \forall k \in \mathcal{K} \tag{13}
$$

where $\mathbf{x}_k$ denotes a zero-mean unit-variance complex Gaussian vector with $\mathbf{x}_k \sim \mathcal{CN}(0, \mathbf{I}_N)$ and

$$
\begin{aligned}
c_k &= \sigma_e^2\Gamma_e - \bar{\boldsymbol{\eta}}_k^H\hat{\boldsymbol{\Theta}}_e\bar{\boldsymbol{\eta}}_k \\
\boldsymbol{\Lambda}_k &= \boldsymbol{\Sigma}_k^{1/2}\hat{\boldsymbol{\Theta}}_e\boldsymbol{\Sigma}_k^{1/2} \\
\mathbf{a}_k &= \boldsymbol{\Sigma}_k^{1/2}\hat{\boldsymbol{\Theta}}_e\bar{\boldsymbol{\eta}}_k.
\end{aligned}
$$

The probabilistic constraint (10) can translate into its deterministic form conservatively as follows:

$$
\begin{aligned}
&\mathrm{Tr}\left(\boldsymbol{\Lambda}_k\right) + \sqrt{2\kappa_k}\sqrt{\|\mathrm{vec}\left(\boldsymbol{\Lambda}_k\right)\|^2 + 2\|\mathbf{a}_k\|^2} \\
&\quad + \kappa_k s^+\left(\boldsymbol{\Lambda}_k\right) \leq c_k \quad \forall k \in \mathcal{K}
\end{aligned} \tag{14}
$$

where $\kappa_k = -\ln(\varepsilon_k)$. Clearly, if (14) is tenable, then constraint (7) also holds true. Based on (12) and (14), problem (P2.2) is equivalently given by:

$$
\begin{aligned}
(\mathcal{P}2.5) \quad \min_{\boldsymbol{\Theta}} \quad & \Gamma_e \\
\text{s.t.} \quad & \mathrm{Tr}\left(\boldsymbol{\Lambda}_b\right) - \sqrt{2\kappa_b}\mu_b - \kappa_b\nu_b \geq c_b \\
& \left\| \begin{matrix} \mathrm{vec}\left(\boldsymbol{\Lambda}_b\right) \\ \sqrt{2}\mathbf{a}_b \end{matrix} \right\| \leq \mu_b \\
& \nu_b\mathbf{I}_{(L+N)} + \boldsymbol{\Lambda}_b \succeq \mathbf{0}, \nu_b \geq 0 \\
& \mathrm{Tr}\left(\boldsymbol{\Lambda}_k\right) + \sqrt{2\kappa_k}\mu_k + \kappa_k\nu_k \leq c_k \\
& \left\| \begin{matrix} \mathrm{vec}\left(\boldsymbol{\Lambda}_k\right) \\ \sqrt{2}\mathbf{a}_k \end{matrix} \right\| \leq \mu_k \\
& \nu_k\mathbf{I}_{(L+N)} - \boldsymbol{\Lambda}_k \succeq \mathbf{0}, \nu_k \geq 0 \quad \forall k \in \mathcal{K}, \\
& \boldsymbol{\Theta}_{l,l} \leq 1, \; l \in \mathcal{L} \\
& \boldsymbol{\Theta} \succeq \mathbf{0}
\end{aligned}
$$

where μ_b, ν_b, μ_k, and ν_k are slack variables. When Γ_e is fixed, this relaxed problem is a convex SDP problem and easily solved by many existing CVX solvers. Adopting the degraded form of problem (P2.3) , the right-hand side of (5) and (6) are replaced with

$$\boldsymbol{\Phi}_b^H \boldsymbol{\Theta} \boldsymbol{\Phi}_b \le \Upsilon_b$$
$$\max_{k \in \mathcal{K}} \boldsymbol{\Phi}_k^H \boldsymbol{\Theta} \boldsymbol{\Phi}_k \ge \Upsilon_k.$$

In this case, problem (P2.2) can also translate into the following form:

$$\begin{aligned}
(\mathcal{P}2.6) \quad \min_{\boldsymbol{\Theta}} \quad & \Gamma_e \\
\text{s.t.} \quad & \mathrm{Tr}\left(\check{\boldsymbol{\Lambda}}_b\right) + \sqrt{2\kappa_b}\mu_b + \kappa_b \nu_b \le \check{c}_b \\
& \left\| \begin{matrix} \mathrm{vec}\left(\check{\boldsymbol{\Lambda}}_b\right) \\ \sqrt{2}\check{\mathbf{a}}_b \end{matrix} \right\| \le \mu_b \\
& \nu_b \mathbf{I}_L - \check{\boldsymbol{\Lambda}}_b \succeq \mathbf{0}, \nu_b \ge 0 \\
& \mathrm{Tr}\left(\check{\boldsymbol{\Lambda}}_k\right) - \sqrt{2\kappa_k}\mu_k - \kappa_k \nu_k \ge \check{c}_k \\
& \left\| \begin{matrix} \mathrm{vec}\left(\check{\boldsymbol{\Lambda}}_k\right) \\ \sqrt{2}\check{\mathbf{a}}_k \end{matrix} \right\| \le \mu_k \\
& \nu_k \mathbf{I}_L + \check{\boldsymbol{\Lambda}}_k \succeq \mathbf{0}, \nu_k \ge 0 \quad \forall k \in \mathcal{K} \\
& \boldsymbol{\Theta}_{l,l} \le 1, \ l \in \mathcal{L} \\
& \boldsymbol{\Theta} \succeq \mathbf{0}.
\end{aligned}$$

In this problem, the symbols $\check{\boldsymbol{\Lambda}}_b$, $\check{\boldsymbol{\Lambda}}_k$, $\check{\mathbf{a}}_b$, $\check{\mathbf{a}}_k$, $\check{c}_b$, and $\check{c}_k$ have similar meanings as $\boldsymbol{\Lambda}_b$, $\boldsymbol{\Lambda}_k$, $\mathbf{a}_b$, $\mathbf{a}_k$, c_b, and c_k in (P2.5). Generally, the solution to this relaxed problem may not be of rank-one. In this case, an approximate rank-one solution θ* to the original optimization problem (P2.1) can be recovered through the standard Gaussian randomization method [31].

7. NUMERICAL RESULTS

This section attempts to confirm the feasibility and the achievable secrecy performance gain for the proposed strategy of IRS-based backscatter jamming by numerical simulations. For comparison, the familiar IRS-based beamforming scheme and the cooperative jamming scheme are also presented as counterparts. This report will investigate how the transmit power P_a at Alice, the element number L of IRS, the distancedfrom the IRS to Bob and the number K of Eves affect Γ_e denoting the maximum SINR of Eves in the case of perfect CSI or the outage SINR of Eves in the case of imperfect CSI. In simulation figures, the legends "Back, Refle, and Coop" denote the proposed strategy, the familiar IRS-based beamforming scheme, and the cooperative jamming scheme, respectively. "Elli" denotes the scheme using the worst case bounding method and "Bern" represents the scheme using the Bernstein-type inequality method, respectively.

In simulations, the Alice-Bob, Alice-Eve and Alice-IRS links are set as slow-fading Rayleigh channels and the other channels follow Rician distribution with their Rician factor κ = 2The path losses of all these channels are given by $\mathrm{PL} = \mathrm{PL}_0 - 10\rho \lg(d / d_0)$, where ρ = 2 denotes the path loss exponent and $\mathrm{PL}_0 = -20$ dB is the path loss at $d_0 = 1$ m representing the reference distance, respectively. Since the radio signal is reflected only by the front half-sphere of IRS, there is 3 dBi gain for all elements. Some other parameters are listed as follows: the distances from Alice to Bob and from the IRS to Bob are set as $d_{ab} = 60$ m and $d_{ib} = 20$m respectively, while the distances from Alice to Eve and from the IRS to Eve satisfy $d_{ae} \sim U(d_{ab} - 5, d_{ab} + 5)$ and $d_{ie} \sim U(d_{ib} - 4, d_{ib} + 4)$, respectively; the distance d_{ai} from Alice to Eve is given by $d_{ai} \sim U(d_{ab} - 5, d_{ab} + 5)$; the antenna number of Alice is

N=4;the noise variances at Bob and Eve are set as $\sigma_b^2 = \sigma_e^2 = 1/(10d_{ab})^2$; the transmit power and the antenna number of cooperative jammer are Pc=0.01 W or 0.03 W and M=4 , respectively, and the jammer has the same location as the IRS. When CSI is perfect, the SINR floor for guaranteeing the reliable communication at Bob is set as $\Gamma_b = 0.9\times|\mathbf{h}_b^H\mathbf{w}|^2/\sigma_b^2$. When CSI is imperfect, the outage SINR at Bob is set as $\Gamma_b = 0.9\times|\bar{\mathbf{h}}_b^H\mathbf{w}|^2/\sigma_b^2$

Fig. 2 illustrates the reception performance at Eves with the transmit power at Alice, where the element number of IRS L = 80, the distance from the IRS to Bob d = 20m and the Eve number K = 3 . From Fig. 2, we observe that Γ_e grows up with $P_a$increasing for all schemes, whether CSI is perfect or not. Compared to the familiar IRS-based beamforming scheme and the cooperative jamming scheme, the proposed strategy of IRS-based backscatter jamming is able to suppress the reception performance at Eves more effectively at high P_a.That is because more signal power can be received and modulated as jamming signal with $P_a$increasing. This result confirms the secrecy performance gain achieved by the proposed strategy of IRS-based backscatter jamming, especially at high P_a.We also find the Bernstein-type inequality scheme outperforms the worst case bounding scheme in the case of imperfect CSI. This result demonstrates the superiority of Bernstein-type inequality scheme in optimizing the beamforming design.

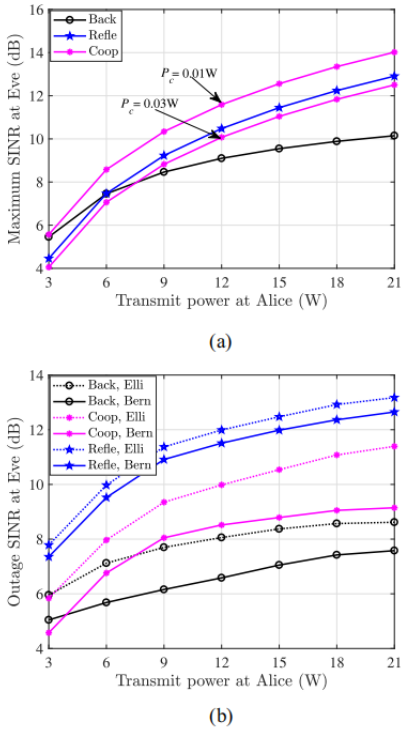

Fig. 2. Reception performance at Eve with respect to the transmit power at Alice, where the element number of IRS $L = 80$, the distance from the IRS to Bob $d = 20$ m and the number of Eves $K = 3$. (a) Maximum SINR Γ_e of Eves in the case of perfect CSI versus the transmit power P_a at Alice. (b) Outage SINR Γ_e of Eves in the case of imperfect CSI versus the transmit power P_a at Alice.

Fig. 3 plots the reception performance at Eves with respect to the element number of IRS, where the transmit power at Alice $P_a = 12W$, the distance from the IRS to Bob d = 20 m and the Eve number K = 3. In Fig. 3, Γe declines with L becoming large for the proposed strategy of IRS-based

backscatter jamming and the familiar IRS-based beamforming scheme, whether CSI is perfect or not. This result shows that the intercepted information amount by Eve is reduced significantly when more elements are printed at the IRS. Moreover, the proposed strategy shows a better performance compared to the familiar IRS-based beamforming scheme in terms of anti-eavesdropping, especially when L is large. That is primarily because the IRS-based beamforming scheme only can reduce confidential signal strength. Instead, the proposed strategy can deteriorate the reception at Eve. By comparing the proposed strategy with the cooperative jamming scheme, it is easily found that using IRS to backscatter jamming signal has the same effect in terms of the reception suppression at Eves as cooperative jamming consuming certain power. Consistent with Fig. 2, the Bernstein-type inequality scheme presents a better performance gain than the worst case bounding scheme in the case of imperfect CSI. All these results indicate that it may be more effective to generate and backscatter jamming rather than reflect the confidential signal directly, when P_a is large. Moreover, the proposed strategy of IRS-based backscatter jamming can achieve the same secrecy performance as the cooperative jamming scheme, with no additional jamming power required.

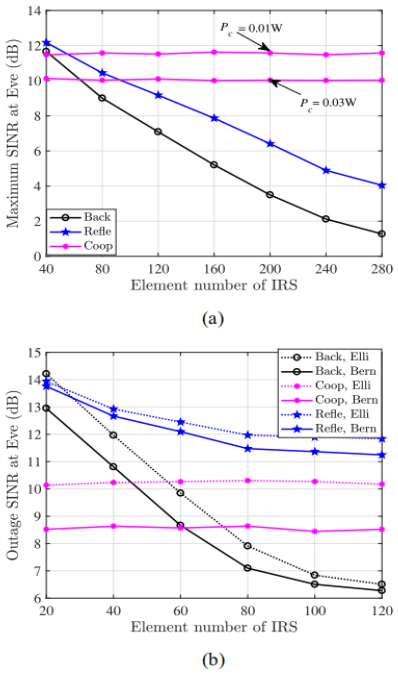

Fig. 3. Reception performance at Eves with respect to the element number of IRS, where the transmit power at Alice $P_a = 12$ W, the distance from the IRS to Bob $d = 20$ m and the number of Eves $K = 3$. (a) Maximum SINR Γ_e of Eves in the case of perfect CSI versus the element number L of IRS. (b) Outage SINR Γ_e of Eves in the case of imperfect CSI versus the element number L of IRS.

Fig. 4 plots the reception performance at Eves with respect to the distance from the IRS to Bob, where the transmit power at Alice $P_a = 12W$, the element number of IRS L = 80 and the Eve number K = 3. From Fig. 4, we find that Γe rises with d becoming large for all curves, whether CSI is perfect or not. The reason is that path loss heavily depends on d. When d is large, the large-scale fading from the IRS to Bob and Eve grows up rapidly. In this case, the received signal power from the IRS at Bob and Eves becomes week, thus reducing the assist effectiveness of IRS. This simulation

result shows that an increase in d is harmful to the secrecy performance. On the other hand, the proposed strategy has a lower Γ_e than the familiar IRS-based beamforming scheme. Compared to the cooperative jamming scheme, IRS-based backscatter jamming signal may achieve a better secrecy performance gain, which is dependent on the element number and the jamming power. Consistent with Figs.2-4 show that the Bernstein-type inequality scheme is superior to the worst case bounding scheme in the case of imperfect CSI

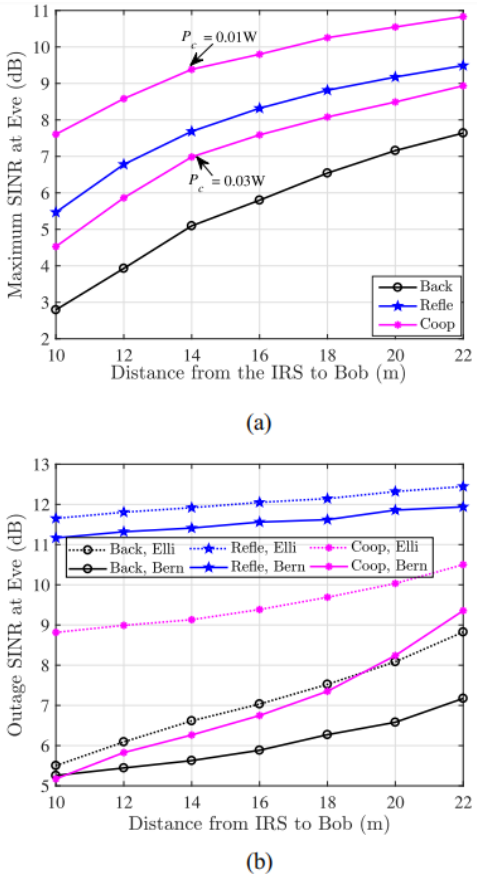

Fig. 4. Reception performance at Eves with respect to the distance from the IRS to Bob, where the transmit power at Alice $P_a = 12$ W, the element number of IRS $L = 80$ and the number of Eves $K = 3$. (a) Maximum SINR Γ_e of Eves in the case of perfect CSI versus the distance d from the IRS to Bob. (b) Outage SINR Γ_e of Eves in the case of imperfect CSI versus the distance d from the IRS to Bob.

Fig. 5 plots the reception performance at Eves with respect to the number of Eves, where the transmit power at Alice $P_a = 12W$, the element number of IRS L = 80 and the distance from the IRS to Bob d = 20m. From Fig. 5, Γ_e rises as K becomes large, whether CSI is perfect or not. The reason is pretty obvious: more Eves mean higher probability in intercepting confidential information due to Eve diversity. By comparison, we find that the proposed strategy achieves a higher secrecy performance gain than the familiar IRS-based beamforming scheme and the cooperative jamming scheme.

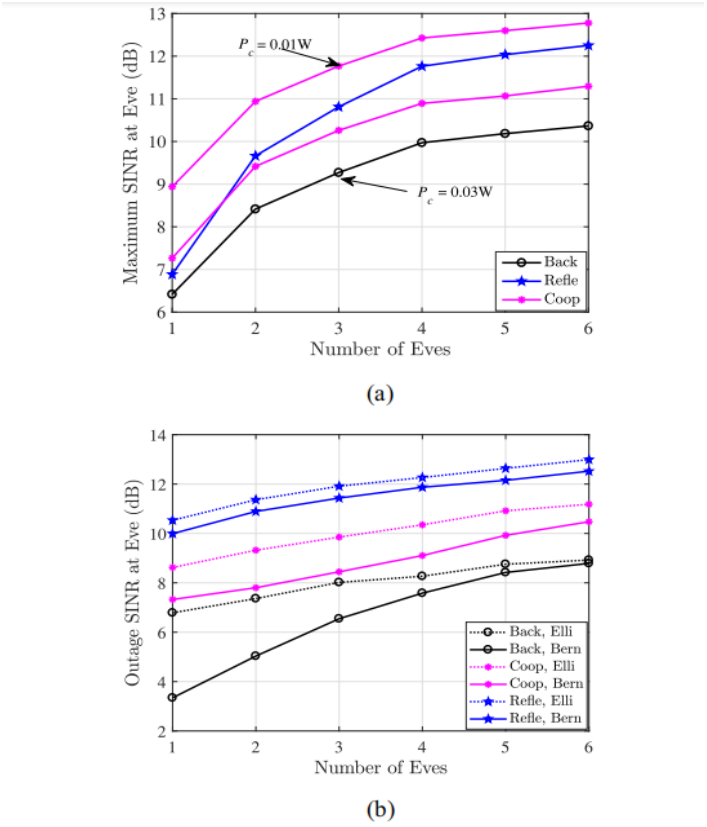

Fig. 5. Reception performance at Eves with respect to the number of Eves, where the transmit power at Alice $P_a = 12$ W, the element number of IRS $L = 80$ and the distance from the IRS to Bob $d = 20$ m. (a) Maximum SINR Γ_e of Eves in the case of perfect CSI versus the number K of Eves. (b) Outage SINR Γ_e of Eves in the case of imperfect CSI versus the number K of Eves.

8. CONCLUSION

This report proposed a strategy of IRS-based backscatter jamming, in which IRS is integrated with backscatter communication. Through spatial modulation, confidential signal from Alice was reflected by IRS in the form of jamming signal. Extensive simulations showed that: 1) the proposed strategy often outperforms the conventional IRS-aided beamforming scheme and the cooperative jamming scheme in the considered system setting; 2) it helps enhance the secrecy performance to coat more elements on IRS and reduce the distance from the IRS to Bob; 3) more confidential signal can be intercepted by Eves with the transmit power at Alice increasing; and 4) more Eves burking around Bob go against the secrecy. Above all, this report provided researchers with a new perspective in IRS-aided PLS. To be specific, the IRS can improve the security by transforming confidential signal into jamming signal in addition to signal cancellation.

REFERENCES

1. S. Han, S. Xu, W.-X. Meng, and L. He, "Channel-correlation-enabled transmission optimization for MISO wiretap channels," IEEE Trans. Wireless Commun., vol. 20, no. 2, pp. 858–870, Feb. 2021.
2. S. Xu, S. Han, W. Meng, and L. He, "QoS-based robust cooperative jamming-aided beamforming for correlated wiretap channels," IEEE Signal Process. Lett., vol. 27, pp. 216–220, Jan. 2020.
3. Y. Du, C. Jiang, J. Wang, Y. Ren, and M. Debbah, "Machine learning for 6G wireless networks: Carrying forward enhanced bandwidth, massive access, and ultrareliable/low-latency service," IEEE Veh. Technol. Mag., vol. 15, no. 4, pp. 122–134, Dec. 2020.

4. S. Han, Y. Huang, W. Meng, C. Li, N. Xu, and D. Chen, "Optimal power allocation for SCMA downlink systems based on maximum capacity," IEEE Trans. Commun., vol. 67, no. 2, pp. 1480–1489, Feb. 2019.
5. H. Hashida, Y. Kawamoto, and N. Kato, "Intelligent reflecting surface placement optimization in air-ground communication networks toward 6G," IEEE Wireless Commun., vol. 27, no. 6, pp. 146–151, Dec. 2020, doi: 10.1109/MWC.001.2000142.
6. S. Xu, J. Liu, Y. Cao, J. Li, and Y. Zhang, "Intelligent reflecting surface enabled secure cooperative transmission for satellite-terrestrial integrated networks," IEEE Trans. Veh. Technol., vol. 70, no. 2, pp. 2007–2011, Feb. 2021.
7. X. Yu, D. Xu, Y. Sun, D. W. K. Ng, and R. Schober, "Robust and secure wireless communications via intelligent reflecting surfaces," IEEE J. Sel. Areas Commun., vol. 38, no. 11, pp. 2637–2652, Nov. 2020.
8. Y. Liu, H.-H. Chen, and L. Wang, "Physical layer security for next generation wireless networks: Theories, technologies, and challenges," IEEE Commun. Surveys Tuts., vol. 19, no. 1, pp. 347–376, 1st Quart., 2017.
9. S. Xu, S. Han, W.-X. Meng, Y. Du, and L. He, "Multiple-jammer-aided secure transmission with receiver-side correlation," IEEE Trans. Wireless Commun., vol. 18, no. 6, pp. 3093–3103, Jun. 2019.
10. Yildirim, A. Uyrus, and E. Basar, "Modeling and analysis of reconfigurable intelligent surfaces for indoor and outdoor applications in future wireless networks," IEEE Trans. Commun., vol. 69, no. 2, pp. 1290–1301, Feb. 2021, doi: 10.1109/TCOMM.2020.3035391.
11. S. Han, Y. Zhang, W. Meng, C. Li, and Z. Zhang, "Full-duplex relay assisted macro cell with millimeter wave backhauls: Framework and prospects," IEEE Netw., vol. 33, no. 5, pp. 190–197, Sep./Oct. 2019.
12. H. Shen, W. Xu, S. Gong, Z. He, and C. Zhao, "Secrecy rate maximization for intelligent reflecting surface assisted multi-antenna communications," IEEE Commun. Lett., vol. 23, no. 9, pp. 1488–1492, Sep. 2019.
13. M. Cui, G. Zhang, and R. Zhang, "Secure wireless communication via intelligent reflecting surface," IEEE Wireless Commun. Lett., vol. 8, no. 5, pp. 1410–1414, Oct. 2019.
14. H.-M. Wang, J. Bai, and L. Dong, "Intelligent reflecting surfaces assisted secure transmission without eavesdropper's CSI," IEEE Signal Process. Lett., vol. 27, pp. 1300–1304, Jul. 2020.
15. V. Liu, A. Parks, V. Talla, S. Gollakota, D. Wetherall, and J. R. Smith, "Ambient backscatter: Wireless communication out of thin air," in Proc. ACM Spec. Interest Group Data Commun. (SIGCOMM), Hong Kong, 2013, pp. 39–50.
16. S. Xu, J. Liu, and J. Zhang, "Resisting undesired signal through IRS-based backscatter communication system," IEEE Commun. Lett., early access, May 3, 2021, doi: 10.1109/LCOMM.2021.3077093.
17. S. Y. Park and D. In Kim, "Intelligent reflecting surface-aided phase shift backscatter communication," in Proc. 14th Int. Conf. Ubiquitous Inf. Manage. Commun. (IMCOM), Taichung, Taiwan, 2020, pp. 1–5.
18. W. Yan, X. Yuan, and X. Kuai, "Passive beamforming and information transfer via large intelligent surface," IEEE Wireless Commun. Lett., vol. 9, no. 4, pp. 533–537, Apr. 2020.
19. W. Zhao, G. Wang, S. Atapattu, T. A. Tsiftsis, and C. Tellambura, "Is backscatter link stronger than direct link in reconfigurable intelligent surface-assisted system?" IEEE Commun. Lett., vol. 24, no. 6, pp. 1342–1346, Jun. 2020.
20. X. Guan, Q. Wu, and R. Zhang, "Joint power control and passive beamforming in IRS-assisted spectrum sharing," IEEE Commun. Lett., vol. 24, no. 7, pp. 1553–1557, Jul. 2020.
21. H. Guo and J. Liu, "UAV-enhanced intelligent offloading for Internet of Things at the edge," IEEE Trans. Ind. Informat., vol. 16, no. 4, pp. 2737–2746, Apr. 2020.
22. S. Zhang, J. Liu, H. Guo, M. Qi, and N. Kato, "Envisioning device-to-device communications in 6G," IEEE Netw., vol. 34, no. 3, pp. 86–91, May/Jun. 2020.
23. Y. Sun, J. Liu, J. Wang, Y. Cao, and N. Kato, "When machine learning meets privacy in 6G: A survey," IEEE Commun. Surveys Tuts., vol. 22, no. 4, pp. 2694–2724, 4th Quart., 2020.
24. C. Huang, A. Zappone, G. C. Alexandropoulos, M. Debbah, and C. Yuen, "Reconfigurable intelligent surfaces for energy efficiency in wireless communication," IEEE Trans. Wireless Commun., vol. 18, no. 8, pp. 4157–4170, Aug. 2019.
25. H. Zhang, B. Di, L. Song, and Z. Han, "Reconfigurable intelligent surfaces assisted communications with limited phase shifts: How many phase shifts are enough?" IEEE Trans. Veh. Technol., vol. 69, no. 4, pp. 4498–4502, Apr. 2020.
26. B. Di, H. Zhang, L. Li, L. Song, Y. Li, and Z. Han, "Practical hybrid beamforming with finite-resolution phase shifters for reconfigurable intelligent surface based multi-user communications," IEEE Trans. Veh. Technol., vol. 69, no. 4, pp. 4565–4570, Apr. 2020.
27. J. Zhang, Y. Zhang, C. Zhong, and Z. Zhang, "Robust design for intelligent reflecting surfaces assisted MISO systems," IEEE Commun. Lett., vol. 24, no. 10, pp. 2353–2357, Oct. 2020.
28. G. Zhou, C. Pan, H. Ren, K. Wang, M. Di Renzo, and A. Nallanathan, "Robust beamforming design for intelligent reflecting surface aided MISO communication systems," IEEE Wireless Commun. Lett., vol. 9, no. 10, pp. 1658–1662, Oct. 2020.

29. L. Dong and H.-M. Wang, "Secure MIMO transmission via intelligent reflecting surface," IEEE Wireless Commun. Lett., vol. 9, no. 6, pp. 787–790, Jun. 2020.
30. B. Li, Z. Fei, Z. Chu, F. Zhou, K.-K. Wong, and P. Xiao, "Robust chance-constrained secure transmission for cognitive satellite–terrestrial networks," IEEE Trans. Veh. Technol., vol. 67, no. 5, pp. 4208–4219, May 2018.
31. Z. Q. Luo, W.-K. Ma, A. M.-C. So, Y. Ye, and S. Zhang, "Semidefinite relaxation of quadratic optimization problems," IEEE Signal Process. Mag., vol. 27, no. 3, pp. 20–34, May 2010.
32. S. Boyd and L. Vandenberghe, Convex Optimization. Cambridge, U.K.: Cambridge Univ. Press, 2004.
33. I. Bechar, "A Bernstein-type inequality for stochastic processes of quadratic forms of Gaussian Variables," Mathematics, 2009.